

Antonio C. O. Miranda,<sup>1</sup> Marco A. Meggiolaro,<sup>1</sup> Jaime T. P. Castro,<sup>1</sup>  
Luiz F. Martha,<sup>1</sup> and Tulio N. Bittencourt<sup>2</sup>

## Fatigue Crack Propagation under Complex Loading in Arbitrary 2D Geometries

---

**Reference:** Miranda, A. C. O., Meggiolaro, M. A., Castro, J. T. P., Martha, L. F., and Bittencourt, T. N., “**Fatigue Crack Propagation under Complex Loading in Arbitrary 2D Geometries,**” *Applications of Automation Technology in Fatigue and Fracture Testing and Analysis: Fourth Volume, ASTM STP 1411*, A. A. Braun, P. C. McKeighan, A. M. Nicolson, and R. D. Lohr, Eds., American Society for Testing and Materials, West Conshohocken, PA, 2002.

**Abstract:** A reliable and cost effective two-phase methodology is proposed and implemented in two pieces of software to predict fatigue crack propagation in generic two-dimensional structural components under complex loading. First, the fatigue crack path and its stress intensity factor are calculated in a specialized finite-element software, using small crack increments. At each crack propagation step, the mesh is automatically redefined based on a self-adaptive strategy that takes into account the estimation of the previous step stress analysis numerical errors. Numerical methods are used to calculate the crack propagation path, based on the computation of the crack incremental direction, and the stress-intensity factors  $K_I$ , from the finite element response. An application example presents a comparison between numerical simulation results and those measured in physical experiments. Then, an analytical expression is adjusted to the calculated  $K_I(a)$  values, where  $a$  is the length along the crack path. This  $K_I(a)$  expression is used as an input to a powerful general purpose fatigue design software based in the local approach, developed to predict both initiation and propagation fatigue lives under complex loading by all classical design methods, including the  $S-N$ , the  $\epsilon-N$  and the  $IIW$  (for welded structures) to deal with crack initiation, and the  $da/dN$  to treat propagation problems. In particular, its crack propagation module accepts any  $K_I$  expression and any  $da/dN$  rule, using a  $\Delta K_{rms}$  or a cycle-by-cycle propagation method to deal with one and two-dimensional crack propagation under complex loading. If requested, this latter method may include overload-induced crack retardation effects.

**Keywords:** fatigue crack propagation, finite elements, arbitrary loading

---

<sup>1</sup> Ph.D. Student – Dept. of Civil Engineering, Research Scientist – Dept. of Mechanical Engineering, Associate Professor – Dept. of Mechanical Engineering, and Associate Professor – Dept. of Civil Engineering, respectively, Pontifical Catholic University of Rio de Janeiro (PUC-Rio), Rua Marquês de São Vicente 225, Rio de Janeiro, RJ – zip code 22453-900 – Brazil

<sup>2</sup> Associate Professor – Dept. of Structural and Foundations Engineering, Polytechnic School at the University of São Paulo (EPUSP), PO Box 61548 – São Paulo, SP – zip code 05424-970 – Brazil

## Introduction

The fatigue crack propagation life prediction under complex loading in intricate two-dimensional (2D) structural components is a quite interesting modeling problem, requiring a mixed approach to achieve its optimum solution.

To predict the crack path and to calculate its associated stress intensity factors  $K_I$  and  $K_{II}$ , a finite element (FE) global discretization of the component, using appropriate crack tip elements, mesh generation schemes and crack increment criteria, has become a common engineering design practice. However, such brute force numerical calculation is not efficient when the load is complex, causing in the general case different crack increments at each load cycle, requiring remeshing and time-consuming recalculations in FE. Moreover, crack retardation effects compromise even more the computational efficiency of this approach.

On the other hand, the local approach, based on the direct integration of the crack propagation rule, can be efficiently used to calculate the crack increment at each load cycle, considering crack retardation effects if necessary. However, it requires as input the stress intensity expression for the crack, which is a major drawback because it is simply not available for most real components. Therefore, designers must use engineering common sense to choose approximate  $K_I$  handbook expressions to solve real problems. The error involved in such approximations obviously increases as the real crack deviates from the modeled crack, and in such cases the accuracy of the local approach is questionable and its predictions unreliable.

Since the advantages of the two approaches are complementary, the problem can be successfully divided into two steps. First, an appropriate FE software can be used to calculate the (generally curved) crack path and its associated Mode I stress intensity factor  $K_I(a)$  along the crack length  $a$ , under **simple** loading. Then, an analytical expression should be adjusted to the discrete  $K_I(a)$  calculated values, to be used as input to a local approach software. Finally, the actual **complex** loading can be efficiently treated by the direct integration of the crack propagation rule, considering retardation effects if required.

This is a simple and evident idea, but it is easier said than implemented, since FE experts are normally not fatigue design engineers, and vice-versa. Moreover, to achieve an engineering tool status, a two-step system must be numerically reliable, simple-to-use, versatile (since there is no universally accepted design method), and, of course, economic. All these constraints put a significant burden on the programming effort.

The purpose of this paper is to describe the fundamentals of an integrated system composed of two complementary programs, designed to implement this two-step method. This system demonstrates that satisfactory fatigue life predictions under complex load for 2D structural components can now be obtained on a PC platform.

The paper is organized in several sections describing (i) the numerical procedures to compute stress intensity factors in arbitrary 2D geometries; (ii) the principles of the crack increment direction numerical computation problem; (iii) a summary of the main features of the FE software developed to handle these tasks, named **QUEBRA2D**; (iv) an experimental verification of the predictions made by this software; (v) the fundamentals of the local approach to predict fatigue life under complex load; (vi) the main features of the **ViDa** software developed to perform such predictions; (vii) the fundamentals of

the  $\Delta K_{rms}$  method numerical implementation for 1D and 2D crack growth; (viii) the principles of the cycle-by-cycle method numerical implementation for 1D and 2D crack propagation; (ix) the minimum number of features required for modeling the load cycle interaction problems; and finally (x) a conclusion.

### Numerical Computation of Stress-Intensity Factors

In 2D finite element models, three methods can be chosen to compute the stress-intensity factors along the (generally curved) crack path: the displacement correlation technique (*DCT*) [1], the potential energy release rate computed by means of a modified crack-closure integral technique (*MCC*) [2, 3], and the *J*-integral computed by means of the equivalent domain integral (*EDI*) together with a mode decomposition scheme [4-8].

#### Displacement Correlation Technique (*DCT*)

In *DCT*, the displacements obtained from the finite element analysis at specific locations are correlated with the analytic solutions expressed in terms of the stress-intensity factors. For quarter-point singular elements [1], the crack opening displacement  $\delta$  is given by

$$\delta(r) = (4v_{j-1} - v_{j-2}) \sqrt{\frac{r}{L}} \quad (1)$$

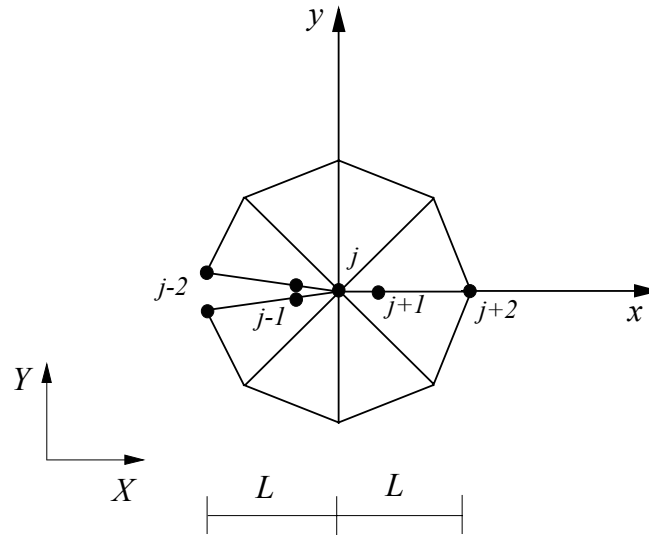


Figure 1 – Quarter-point elements at the crack tip.

where  $v_{j-1}$  and  $v_{j-2}$  are the relative displacements in the *y* direction, at the *j*-1 and *j*-2 nodes, and *L* is the element size (Figure 1). The analytical expression for  $\delta$  is

$$\delta(r) = K_I \left( \frac{\kappa+1}{\mu} \right) \sqrt{\frac{r}{2\pi}} \quad (2)$$

where  $\kappa = 3 - 4\nu$  for plane strain,  $\kappa = (3 - \nu)/(1 + \nu)$  for plane stress,  $\nu$  is the Poisson ratio, and  $\mu$  is the shear modulus. By equating the numerical and the analytical expressions for  $\delta$ , (1) and (2), the Mode I stress-intensity factor can be evaluated by

$$K_I = \left( \frac{\mu}{\kappa + 1} \right) \sqrt{\frac{2\pi}{L}} (4v_{j-1} - v_{j-2}) \quad (3)$$

For Mode II, the crack opening displacement is replaced by the crack sliding displacement and, following the same steps,  $K_{II}$  is calculated by

$$K_{II} = \left( \frac{\mu}{\kappa + 1} \right) \sqrt{\frac{2\pi}{L}} (4u_{j-1} - u_{j-2}) \quad (4)$$

where  $u_{j-1}$  and  $u_{j-2}$  are the relative displacements in the  $x$  direction, at the  $j-1$  and  $j-2$  nodes (Figure 1).

#### *Modified Crack-Closure Integral (MCC)*

The modified crack-closure method is based on the Irwin's crack-closure integral concept, which assumes that the required work to close a crack from  $a + \delta a$  to  $a$  is the same as that required to extend it from  $a$  to  $a + \delta a$  (Figure 2). Based on this assumption, the strain-energy release rates  $G_I$  and  $G_{II}$  of a mixed-mode condition are obtained by

$$G_I = \lim_{\delta a \rightarrow 0} \frac{1}{2\delta a} \int_0^{\delta a} v(r) \sigma_y(r) dr \quad \text{and} \quad G_{II} = \lim_{\delta a \rightarrow 0} \frac{1}{2\delta a} \int_0^{\delta a} u(r) \sigma_{xy}(r) dr \quad (5)$$

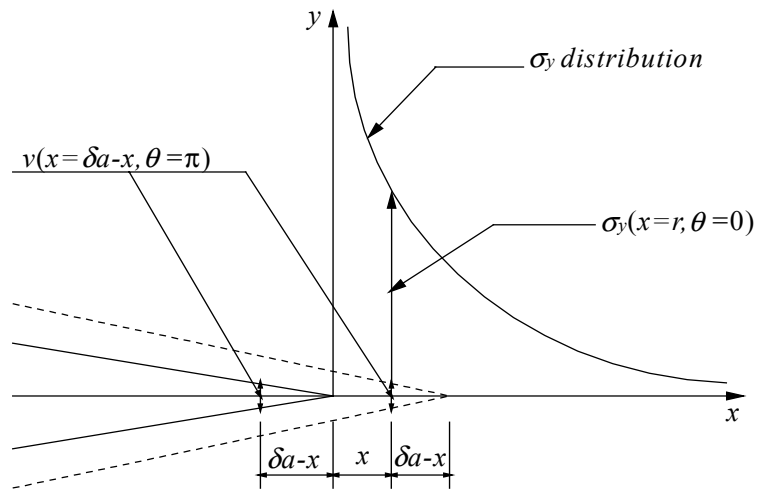


Figure 2 – Analytical crack-closure integral method.

In these equations,  $\delta a$  is the virtual crack extension;  $\sigma_y$  and  $\sigma_{xy}$  are the normal and shear stress distributions ahead of the crack tip; and  $v(r)$  and  $u(r)$  are the crack opening and sliding displacements at a distance  $r$  behind the new crack tip. In the original form, the results are obtained from two analyses: one with a crack length  $a$  and the other with a crack length  $a + \delta a$ .

Rybicki and Kanninen [2] were the first to use this approach with a single finite element analysis, using models with four-noded quadrilateral elements. Raju [3] extended this method for non-singular and singular elements of any order. This procedure is based on the symmetry of the elements around the crack tip. In the numerical computation of  $G_I$  and  $G_{II}$ , the strain-energy release rates given by Equation 5, the stress field is assumed to have the classical  $1/\sqrt{r}$  distribution and the displacements  $u(r)$  and  $v(r)$  are determined by interpolation of nodal displacements using the element shape functions. The normal and shear stresses are obtained from the nodal forces at and ahead of the crack tip.

As shown by Raju [3], simplified expressions for singularity elements may be applied, which are easier to use than the consistent expressions. The components  $G_I$  and  $G_{II}$  for pure Mode I and Mode II, and for mixed mode conditions are given as

$$G_I = -\frac{1}{2\delta a} \left[ F_{y_i} \{t_{11}(v_m - v_{m'}) + t_{12}(v_l - v_{l'})\} + F_{y_j} \{t_{21}(v_m - v_{m'}) + t_{22}(v_l - v_{l'})\} \right] \quad (6)$$

$$G_{II} = -\frac{1}{2\delta a} \left[ F_{x_i} \{t_{11}(u_m - u_{m'}) + t_{12}(u_l - u_{l'})\} + F_{x_j} \{t_{21}(u_m - u_{m'}) + t_{22}(u_l - u_{l'})\} \right] \quad (7)$$

where  $F_{x_i}$ ,  $F_{x_j}$ ,  $F_{y_i}$ , and  $F_{y_j}$  are the consistent nodal forces acting on nodes  $i$  and  $j$  in the  $x$  and  $y$  directions (Figure 3);  $u$  and  $v$  are the nodal displacements at  $m$ ,  $m'$ ,  $l$  and  $l'$  nodes in the  $x$  and  $y$  directions, respectively; and  $t_{11} = 6 - 3\pi/2$ ,  $t_{12} = 6\pi - 20$ ,  $t_{21} = 1/2$ , and  $t_{22} = 1$ . The nodes and nodal forces  $F_{y_i}$  and  $F_{y_j}$  are shown in Figure 3.

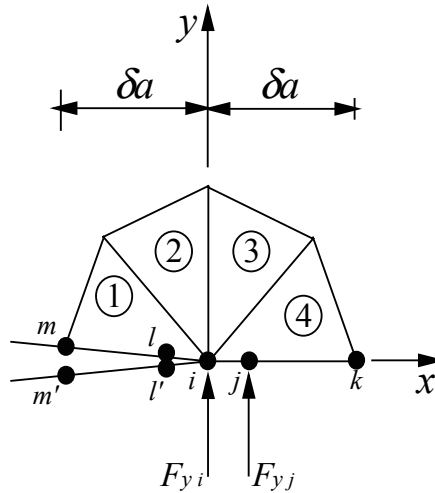


Figure 3 – Node at crack tip elements and consistent nodal forces ahead of crack tip.

The nodal forces  $F_{x_i}$  and  $F_{y_i}$  are computed from elements 1, 2, 3 and 4, but the forces  $F_{x_j}$  and  $F_{y_j}$  are computed from element 4 only. Under linear elastic conditions (LEFM), the stress-intensity factors are related to the energy release rates by

$$G_I = \frac{\kappa+1}{8\mu} K_I^2 \quad \text{and} \quad G_{II} = \frac{\kappa+1}{8\mu} K_{II}^2 \quad (8)$$

where  $\kappa$  has been previously defined for plane stress and plane strain conditions. It is assumed that the classical ASTM E399 requirements for validating a  $K_{IC}$  toughness test can also be used in fatigue crack growth to characterize a plane strain condition.

### *J-Integral Formulation with Equivalent Domain Integral (EDI)*

The  $J$ -integral is a path independent contour integral introduced by Rice [9] to study non-linear elastic materials under small scale yielding. The equivalent domain integral method replaces the integration along the contour by another one over a finite size domain, using the divergence theorem. This definition is more convenient for finite element analysis. For two-dimensional problems, the contour integral is replaced by an area integral

$$J = - \int_A \left[ W \frac{\partial q}{\partial x} - \sigma_{ij} \frac{\partial u_i}{\partial x} \frac{\partial q}{\partial x} \right] dA - \int_A \left\{ \frac{\partial W}{\partial x} - \frac{\partial}{\partial x} \left[ \sigma_{ij} \frac{\partial u_i}{\partial x} \right] \right\} q dA - \int_S t_i \frac{\partial u_i}{\partial x} q ds \quad (9)$$

where  $W$  is the strain energy density;  $q$  is a continuous function that allows for the equivalent domain integral to be treated in the finite element formulation;  $\sigma_{ij}$  are the stresses at the contour  $C$ , which is any path surrounding the crack tip;  $u_i$  are the displacements correspondent to local  $i$ -axes;  $t_i$  is the crack face pressure load, and  $s$  is the arc length of the contour. Usually, a linear function is chosen for  $q$ , which assumes a unit value at the crack tip and a null value along the contour. For the linear-elastic materials special case, the second term in Equation 9 vanishes. The third term will vanish if the crack faces are not loaded, or if  $q = 0$  at the loaded portions of the crack faces.

The  $J$ -integral definition considers a balance of mechanical energy for a virtual translation field along the  $x$ -axis. In the case of either pure Mode I or pure Mode II, Equation 9 allows for the calculation of stress-intensity factors  $K_I$  or  $K_{II}$ . However, in the mixed mode case,  $K_I$  and  $K_{II}$  can not be calculated separately from this equation alone. In this case, other invariant integrals are used. Usually, the expression defined by Knowles and Sternberg [10] is adopted

$$J_k = - \int_A \left[ W \frac{\partial q}{\partial x_k} - \sigma_{ij} \frac{\partial u_i}{\partial x_k} \frac{\partial q}{\partial x_j} \right] dA - \int_A \left[ \frac{\partial W}{\partial x_k} - \sigma_{ij} \frac{\partial}{\partial x_j} \left( \frac{\partial u_i}{\partial x_k} \right) \right] q dA - \int_S t_i \frac{\partial u_i}{\partial x_k} q ds \quad (10)$$

where  $k$  is an index for local crack tip axes ( $x, y$ ). These integrals were introduced initially for small deformation [9] and were extended by Atluri [11] for finite deformations.

The integration is performed in the elements chosen to represent the domain. In this work, the chosen domain is the rosette of quarter-point elements at the crack tip (Figure 1), and the standard Gaussian quadrature is used over each element.

For linear elastic problems, Bui [4] proposed associated fields to decompose the loading modes. In this case, the first component in Equation 10 is path independent, but the second one is not. However, the path dependency may be eliminated if the displacements and the stress fields are decomposed into symmetric and anti-symmetric portions. Therefore, the displacement field is rewritten as

$$\begin{aligned} u &= u^I + u^{II} = \frac{1}{2}(u + u') + \frac{1}{2}(u - u') \\ v &= v^I + v^{II} = \frac{1}{2}(v - v') + \frac{1}{2}(v + v') \end{aligned} \quad (11)$$

where  $u$  and  $v$  are displacements in  $x$  and  $y$  directions, respectively,  $u'(x, y) = u'(x, -y)$ , and  $v'(x, y) = v'(x, -y)$ ; and the superscripts  $I$  and  $II$  correspond to the symmetric and anti-symmetric components of the displacements field, respectively. The stress field is then decomposed as

$$\begin{aligned} \sigma_{xx} &= \sigma_{xx}^I + \sigma_{xx}^{II} = \frac{1}{2}(\sigma_{xx} + \sigma'_{xx}) + \frac{1}{2}(\sigma_{xx} - \sigma'_{xx}) \\ \sigma_{yy} &= \sigma_{yy}^I + \sigma_{yy}^{II} = \frac{1}{2}(\sigma_{yy} + \sigma'_{yy}) + \frac{1}{2}(\sigma_{yy} - \sigma'_{yy}) \\ \sigma_{zz} &= \sigma_{zz}^I + \sigma_{zz}^{II} = \frac{1}{2}(\sigma_{zz} + \sigma'_{zz}) \\ \sigma_{xy} &= \sigma_{xy}^I + \sigma_{xy}^{II} = \frac{1}{2}(\sigma_{xy} - \sigma'_{xy}) + \frac{1}{2}(\sigma_{xy} + \sigma'_{xy}) \end{aligned} \quad (12)$$

where  $\sigma'_{ij}(x, y) = \sigma'_{ij}(x, -y)$  and  $\sigma_{zz}^{II} = 0$ .

New integrals  $J_I$  and  $J_{II}$  are obtained, which satisfy the condition  $J = J_I + J_{II}$ , where  $J_I$  is associated to the symmetric field (Mode I) and  $J_{II}$  is associated to anti-symmetric fields (Mode II)

$$J_I = - \int_A \left[ W(u_i^I) \frac{\partial q}{\partial x_k} - \sigma_{ij}(u_i^I) \frac{\partial u_i^I}{\partial x_k} \frac{\partial q}{\partial x_j} \right] dA - \int_S t_i \frac{\partial u_i^I}{\partial x_k} q ds \quad (13)$$

$$J_{II} = - \int_A \left[ W(u_i^{II}) \frac{\partial q}{\partial x_k} - \sigma_{ij}(u_i^{II}) \frac{\partial u_i^{II}}{\partial x_k} \frac{\partial q}{\partial x_j} \right] dA - \int_S t_i \frac{\partial u_i^{II}}{\partial x_k} q ds \quad (14)$$

This approach has also been applied by Atluri et al. [7, 8] with highly accurate results for mixed-mode problems. In addition, Eischen [12], and Kienzler and Kordisch [13] suggested improved methods for obtaining  $J$ -integrals for mixed-mode problems. These modifications and decomposition techniques permit the use of the  $J$ -integral and EDI approaches for a wide range of linear and non-linear deformation crack problems.

In LEFM,  $J$  is equal to the energy release rate  $G$ , and its components  $J_I$  and  $J_{II}$  may be used to compute stress-intensity factors by means of Equation 8.

## Numerical Computation of the Crack Increment Direction

In 2D finite element analysis, the three most used criteria for numeric computation of crack (incremental) growth in the linear-elastic regime are: (a) the maximum circumferential stress ( $\sigma_{\theta_{max}}$ ) [14], (b) the maximum potential energy release rate ( $G_{\theta_{max}}$ ) [15], and (c) the minimum strain energy density ( $S_{\theta_{min}}$ ) [16].

In the first criterion, Erdogan and Sih considered that the crack extension should occur in the direction that maximizes the circumferential stress in the region close to the crack tip [14]. In the second, Hussain et al. [15] have suggested that the crack extension occurs in the direction that causes the maximum fracturing energy release rate. And in the last, Sih [16] assumed that the crack growth direction is determined by the minimum strain energy density value near the crack tip. Bittencourt et al. [17] have shown that, if the crack orientation is allowed to change in automatic fracture simulation, the three criteria furnish basically the same results. Since the maximum circumferential stress criterion is the simplest, it is the criterion described below.

The stresses on the crack tip for Modes I and II are given by summing up the stresses obtained for each mode separately [18]. As a result, the following equations are obtained in polar coordinates

$$\sigma_r = \frac{1}{\sqrt{2\pi r}} \cos(\theta/2) \left\{ K_I \left[ 1 + \sin^2(\theta/2) \right] + \frac{3}{2} K_{II} \sin \theta - 2K_{II} \tan(\theta/2) \right\} \quad (15)$$

$$\sigma_\theta = \frac{1}{\sqrt{2\pi r}} \cos(\theta/2) \left[ K_I \cos^2(\theta/2) - \frac{3}{2} K_{II} \sin \theta \right] \quad (16)$$

$$\tau_{r\theta} = \frac{1}{\sqrt{2\pi r}} \cos(\theta/2) \left[ K_I \sin \theta + K_{II} (3\cos \theta - 1) \right] \quad (17)$$

These expressions are valid both for plane stress and plane strain. The maximum circumferential stress criterion determines that the crack extension begins on a plane perpendicular to the direction in which  $\sigma_\theta$  is maximum, thus  $\tau_{r\theta} = 0$ , and that the monotonic (non-fatigued) extension shall occur when  $\sigma_{\theta_{max}}$  reaches a critical value corresponding to a property of the material ( $K_{IC}$  for Mode I). From Equations 15-17 and  $\tau_{r\theta} = 0$ , it is found a trivial solution  $\theta = \pm \pi$  for  $\cos(\theta/2) = 0$ , and a non-trivial solution

$$K_I \sin \theta + K_{II} (3\cos \theta - 1) = 0 \quad (18)$$

Analyzing Equation 18 for the two pure modes, it is found for pure Mode I that  $K_{II} = 0$ ,  $K_I \sin \theta = 0$ , and  $\theta = 0^\circ$ , and for pure Mode II that  $K_I = 0$ ,  $K_{II} (3\cos \theta - 1) = 0$ , and  $\theta = \pm 75^\circ$ . These  $\theta$  values are the extreme values of the crack propagation angle. The intermediate values are found solving Equation 18 for  $\theta$  considering the mixed mode

$$\theta = 2 \arctan \left( \frac{1}{4} \frac{K_I}{K_{II}} \pm \frac{1}{4} \sqrt{\left( \frac{K_I}{K_{II}} \right)^2 + 8} \right) \quad (19)$$

where the sign of  $\theta$  is the opposite of the sign of  $K_{II}$ .



## Finite Element Crack Propagation Simulation

The computational models described above were implemented in a software called **QUEBRA2D** (meaning 2D fracture in Portuguese) [19, 20], which is an interactive graphical software for simulating two-dimensional fracture processes based on a finite element adaptive mesh generation strategy [21]. The adaptive process first requires the results from the analysis of an initial finite element mesh, usually rough, with the geometric descriptions, the boundary conditions, and their attributes. Then a discretization of the domain's region boundary is performed based on the geometric properties and on the characteristic sizes of the boundary elements, determined from the error estimate resulting from the previous step FE analysis.

It is important to point out that one advantage of this strategy is that the boundary curve is discretized independently from the model's domain, thus resulting in a more regular boundary discretization. From this discretization, the new mesh is generated [22], based on quadtree [23] and Delaunay [24] triangulation techniques. The quadtree generates the mesh in the interior of the model, leaving a band near the boundary to be discretized by the Delaunay triangulation. This process is repeated until the estimate discretization error reaches a predefined value [19, 21].

Some other **QUEBRA2D** highlights are: (i) visualization of iso-strips and iso-lines from scalar results at the nodes and at the Gauss points; (ii) stress-intensity factor and crack propagation direction computation by means of all methods described above; (iii) vectorial or scalar plotting for visualizing the principal stress results; (iv) visualization of the model's deformed configuration, with zoom, distortion, and translation specification; (v) visualization of the model's animation along the several steps; and (vi) option of the interface language.

The software has been implemented in C language, using the IUP/LUA interface system (<http://www.tecgraf.puc-rio.br/manual/iup>) and the CD graphic system (<http://www.tecgraf.puc-rio.br/manual/cd>). This environment allows, without any code modification, automatic portability to several platforms, including workstations based on the Unix operating system and PCs running under Windows 98/2000 or NT.

## Experimental Verification of the Crack Path Prediction

A simple test was performed to verify the crack path predicted by the **QUEBRA2D** software and to demonstrate its capabilities. A crack was fatigue propagated in a SEN specimen with a hole slightly to the left of the starting notch (created using a 0.3mm jeweler's saw), loaded in four-point bending (Figure 4). Due to the hole, the crack does not follow a straight line path, but curves toward the hole.

The material used in the experiment was a 1020 steel (analyzed composition: C 0.19; Mn 0.46; Si 0.14; Ni 0.052; Cr 0.045; Mo 0.007; Cu 0.11; Nb 0.002; Ti 0.002; Fe balance) with Young modulus  $E = 205\text{GPa}$ , yielding strength  $S_Y = 285\text{MPa}$ , ultimate strength  $S_U = 491\text{MPa}$ , and area reduction  $RA = 54\%$ . Two crack growth equations were fitted to experimental data (obtained testing CTS in a servohydraulic test machine under sinusoidal load at 20Hz): the Paris equation, yielding  $da/dN = 8.5 \cdot 10^{-14} \cdot \Delta K^{4.2}$ , and a modified Elber equation,  $da/dN = 4.5 \cdot 10^{-10} \cdot (\Delta K - \Delta K_{th})^{2.1}$ , where the threshold stress intensity range  $\Delta K_{th} = 11.6\text{MPa}\sqrt{m}$ .

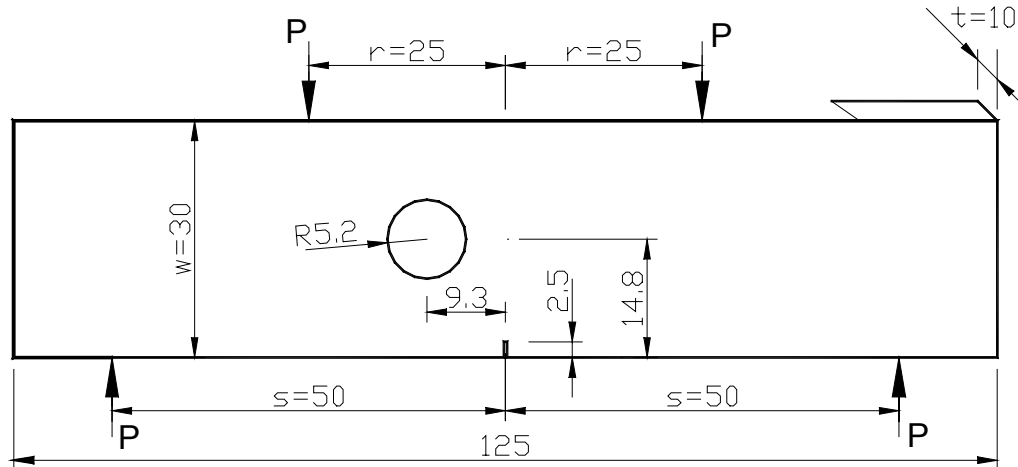


Figure 4 – SEN specimen with a hole to the left of the starting notch (dimensions in mm).

The experiment was performed under constant stress intensity range  $\Delta K = 18.0 \text{ MPa} \sqrt{\text{m}}$  and  $R = 0.1$ . The maximum loads varied from  $11.0 \text{ kN}$  to  $2.8 \text{ kN}$  to keep  $\Delta K$  constant as the crack propagated from  $2.5 \text{ mm}$  to  $16.5 \text{ mm}$  (measured along the crack path).

Figure 5 shows the FE mesh automatically generated for the final crack configuration. Figure 6 compares the predicted crack path with the actual one. The crack path was predicted by the  $\sigma_{\theta_{max}}$  method and  $K_I$  was computed by the MCC technique. For refined meshes such as the one shown in Figure 5, all methods predict essentially the same results, as discussed in [17]. Finally Figure 7 presents the calculated Mode I stress intensity factor along the crack path,  $K_I(a)$ . This is the information that the local approach uses for calculating the fatigue life under complex loading.

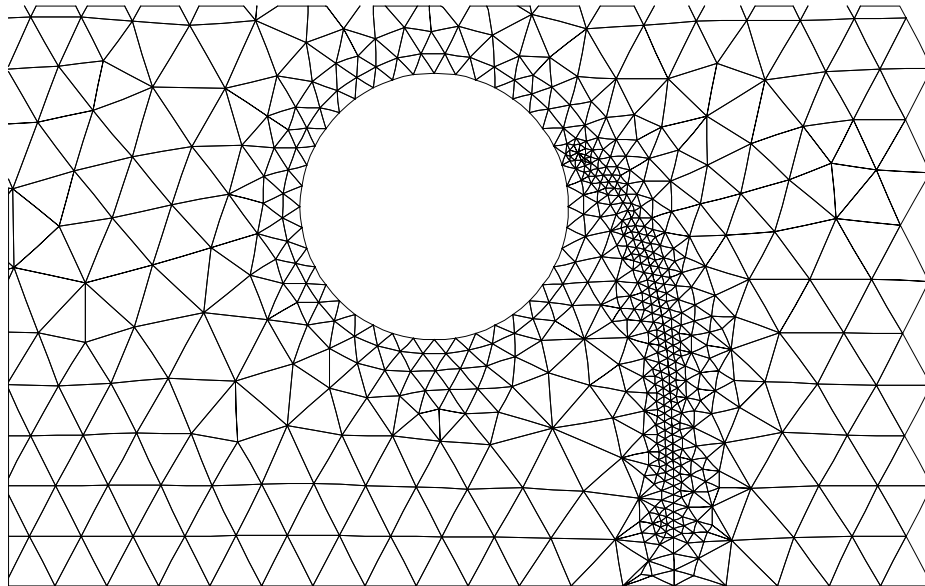


Figure 5 – FE mesh automatically generated for the final crack configuration.

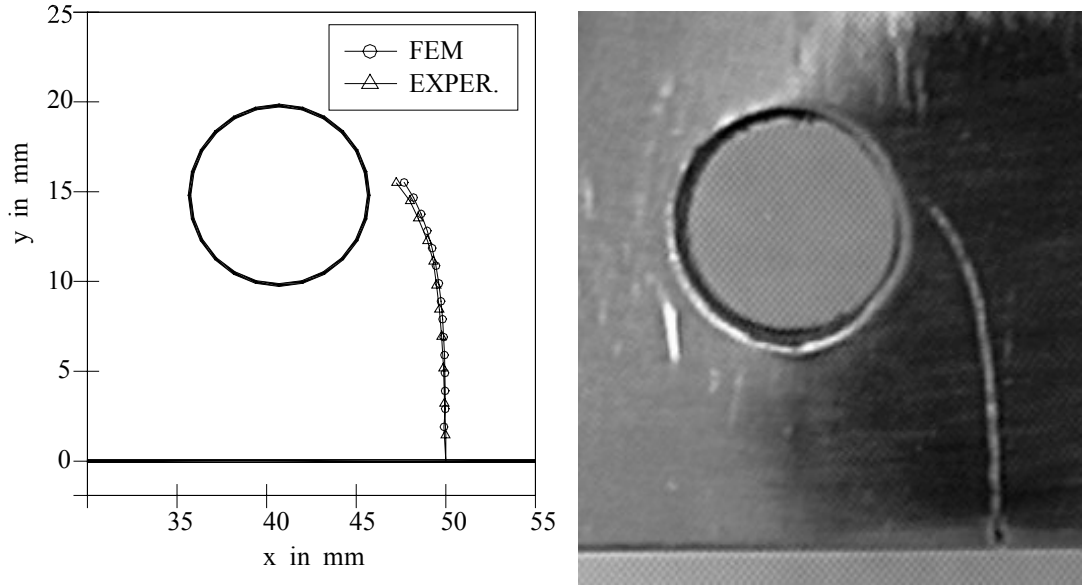


Figure 6 – Predicted and measured crack path.

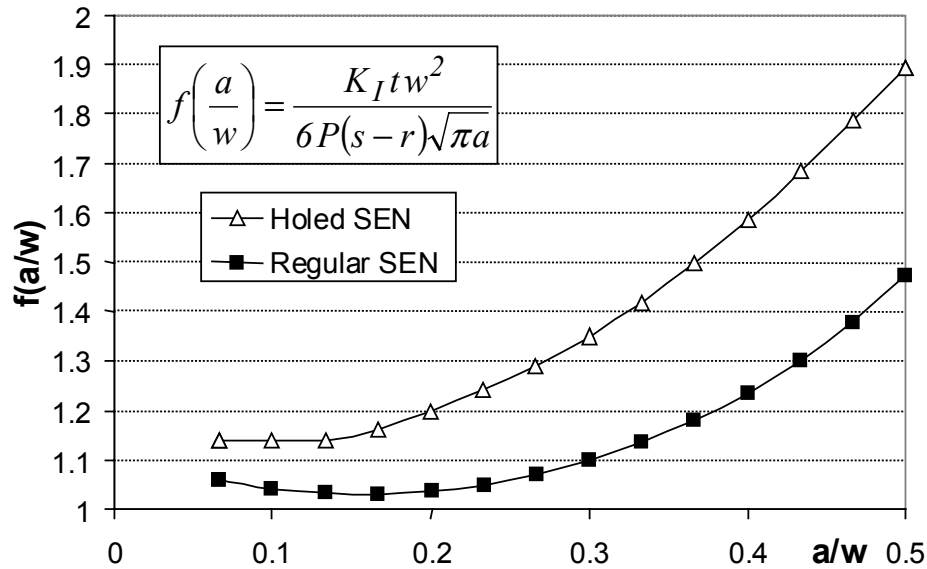


Figure 7 – Calculated  $K_I(a)$  along the crack path for the holed and regular SEN.

### Automation of the Fatigue Crack Propagation Calculation under Complex Loading

The modeling and the calculation automation of the LEFM Mode I fatigue crack propagation under complex loading by the **local** approach are discussed below. Both 1D and 2D cracks are studied, even though these last are not dealt with in the FE modeling discussed above. The loading complexity, whose amplitude can randomly vary in time, is not limited. Sequence effects, such as overload-induced crack retardation or arrest are also considered. Only Mode I is discussed, since fatigue cracks almost always propagate perpendicular to the maximum tensile stress.

The local approach is so-called because it does not require the global solution of the structure's stress field, because it is based on the direct integration of the fatigue crack propagation rule of the material,  $da/dN = F(\Delta K, R, \Delta K_{th}, K_C, \dots)$ , where  $\Delta K$  is the stress intensity range,  $R = K_{min}/K_{max}$  is a measure of the mean load,  $\Delta K_{th}$  is the fatigue crack propagation threshold, and  $K_C$  is the toughness of the material-structure. Appropriate stress intensity factor expression for  $\Delta K$  and  $da/dN$  rule must be used to obtain satisfactory predictions. Therefore, neither the  $\Delta K$  expression nor the type of crack propagation rule should have their accuracy compromised when using this approach.

The interaction with the environment and out-of-phase loading at multiple origins, which induce stresses whose principal directions vary significantly in time, are considered out of the scope of this discussion. In the same way, it does not consider the small crack problem, whose size is of the order of (i) the size parameter that characterizes the intrinsic anisotropy of the material (e.g., grain size), or (ii) the plastic zone associated to the crack tip or to the notch in which the (short) crack is built-in.

In the sequence of this text, first the main features of the software **ViDa** (which means life in Portuguese) are concisely described. This software has been developed to automate all the traditional local approach methods used in fatigue design [25, 26], including the  $S-N$ , the  $IIW$  (for welded structures) and the  $\varepsilon-N$  for crack initiation, and the  $da/dN$  for crack propagation. Then the following topics are discussed: (i) the  $\Delta K_{rms}$  method, including the differences between 1D and 2D crack propagation modeling; (ii) the cycle-by-cycle method, also emphasizing the differences between the 1D and the 2D problems; (iii) some proposals for increasing the computational efficiency of the models; and (iv) the modeling of load sequence effects. Finally, the advantages and limitations of the several studied models are evaluated.

## The **ViDa** Software

The objective of this software is to automate all the calculations required to predict fatigue life under complex loading using the local approach. It runs on PCs under Windows 95 or better operating system, and it includes all the necessary tools to perform the predictions, such as intuitive and friendly graphic interfaces in multiple idioms; intelligent databases for stress concentration and intensity factors, crack propagation rules, material properties, and the like; traditional and sequential rain-flow counters, graphic generators of elastoplastic hysteresis loops and of 2D cracks fronts; automatic adjustment of crack initiation and propagation experimental data; an equation interpreter, etc. The software calculates crack growth considering any propagation rule and any  $\Delta K$  expression that can be written in a BASIC syntax (making it an ideal companion to **QUEBRA2D** software, which can be used to generate the  $\Delta K(a)$  expression if it is not available in its database).

The loading can be given by a sequential list of peaks ( $\sigma_{max}$ ) and valleys ( $\sigma_{min}$ ), or else by the equivalent sequence of the number of reversions ( $n/2$ ) of alternate ( $\sigma_a$ ) and mean ( $\sigma_m$ ) stresses. The loading can also be specified in strain instead of stress. The data can be typed or imported from any text file, including those experimentally generated (e.g. by strain-gages).

The propagation is calculated at each load event. An event is defined by a block of simple load, in which  $\sigma_a$  and  $\sigma_m$  remain constant during  $n$  cycles, or at each variation of the load amplitude in the complex case. In any case, the software automatically stops the calculations, and indicates the value of the parameters that caused the stop, if during the loading it detects that: (i)  $K_{max} = K_C$ ; (ii) the crack reaches its maximum specified size; (iii) the stress in the residual ligament reaches the rupture strength of the material  $S_U$ ; (iv) the crack propagation rate  $da/dN$  reaches 0.1mm/cycle (above this rate fracturing occurs, not fatigue cracking); or (v) one of the borders of the piece is reached by the front of the crack, in the 2D crack propagation case. However, for some geometries, the software is able to calculate 2D crack propagation even after the borders of the piece are reached, by modeling the stress intensity factors of the transition from part-through to through cracks.

Moreover, the software informs when there is yielding in the residual ligament before the maximum specified crack size or number of load cycles is reached. In this way, the calculated values can be used with the guarantee that the limit of validity of the mathematical models is never exceeded.

### The $\Delta K_{rms}$ Method

The stress intensity factor range is expressed as  $\Delta K = \Delta\sigma \cdot [\sqrt{(\pi a)} \cdot f(a/W)]$ , where  $\Delta\sigma$  is the nominal stress range (in relation to which the  $\Delta K$  expression is defined),  $a$  is the crack length,  $f(a/W)$  is a non-dimensional function of  $a/W$ , and  $W$  is a characteristic size of the structure. Therefore,  $\Delta\sigma$  quantifies the influence of the loading and  $\sqrt{(\pi a)} \cdot f(a/W)$  quantifies the effect of the geometry of the piece and of the crack shape and size in  $\Delta K$ .

The simplest way to treat the fatigue life prediction under a complex loading problem is to substitute a simple equivalent loading, causing the same growth of the crack. It has been experimentally discovered that  $\Delta K_{rms}$ , the root mean square value of the stress intensity range, can in some cases be used for this purpose [18].

According to Hudson [27],  $\Delta K_{rms}$  can be calculated from the *rms* values of the positive peaks and valleys of the loading (since the crack does not grow while closed, the compressive part of the loading should be discarded). Therefore

$$\sigma_{max_{rms}} = \sqrt{\frac{1}{p} \sum_{i=1}^p (\sigma_{max_i})^2} \quad \text{and} \quad \sigma_{min_{rms}} = \sqrt{\frac{1}{q} \sum_{i=1}^q (\sigma_{min_i})^2}, \quad (\sigma_{max_i}, \sigma_{min_i} \geq 0) \quad (20)$$

$$\Delta\sigma_{rms} = \sigma_{max_{rms}} - \sigma_{min_{rms}} \quad \text{and} \quad R_{rms} = \frac{\sigma_{min_{rms}}}{\sigma_{max_{rms}}} \quad (21)$$

As  $\Delta K_{rms} = \Delta\sigma_{rms} \cdot [\sqrt{(\pi a)} \cdot f(a/W)]$ , the number of cycles the crack takes to grow from the initial length  $a_0$  to the final one  $a_f$  is given by

$$N = \int_{a_0}^{a_f} \frac{da}{F(\Delta K_{rms}, R_{rms}, \Delta K_{th}, K_C, \dots)} \quad (22)$$

In the **ViDa** software, a variation of the Simpson's algorithm can be used for the numerical integration of the simple loading case and, consequently, also for the  $\Delta K_{rms}$  method. Crack increments  $\delta a > 0.1 \mu\text{m}$  for the discretization of the integral can be specified by the user, who can also choose an integration method based on adjustable steps depending on the variation of the crack length, as will be discussed later on the study of the cycle-by-cycle method.

It should be mentioned that the  $\Delta K_{rms}$  value of a complex loading is similar but not identical to the  $\Delta K$  of a simple loading. As with any statistics,  $\Delta K_{rms}$  does not recognize temporal order, and cannot detect some important problems such as: sudden fracture caused by a single large peak during the complex loading (in order to start the fracture process, it is enough that in just **one** event  $K_{max} = K_C$ ); or any interaction among the loading cycles (e.g. the crack retardation or arrest phenomena after an overload). Also, it is **not** possible to guarantee the inactivity of the crack if  $\Delta K_{rms}(a_0) < \Delta K_{th}(R_{rms})$ .

In complex loading, this latter problem can be caused by all the  $(\Delta\sigma_i, R_i)$  events that induce  $\Delta K_i > \Delta K_{th}(R_i)$ , which can make the crack grow even if  $\Delta K_{rms} < \Delta K_{th}(R_{rms})$ . Therefore, as  $\Delta K_i$  depends both on the stress range  $\Delta\sigma_i$  and on the crack size  $a_i$  in that event, even if the value of  $\Delta\sigma_{rms}$  stays constant, the same cannot be guaranteed for  $\Delta K_{rms}$ .

### *The $\Delta K_{rms}$ Method for 2D Cracks*

Equation 22 can only be applied to 1D cracks, but in practice many times it is necessary to study surface, corner, or internal cracks that propagate in 2D. The principal characteristic of these cracks is a non-homologous fatigue propagation: in general, the crack front tends to change form from cycle to cycle, because  $\Delta K$  varies from point to point along the crack front.

There are analytical expressions for the stress intensity factor of some 2D cracks. If the cracks have ellipsoidal fronts built in a plate of width  $W$  or  $2W$  and thickness  $t$ ,  $\Delta K$  is function of  $\Delta\sigma$ ,  $a$ ,  $a/c$ ,  $a/t$ ,  $c/W$  and  $\theta$  [28-30], where  $a$  and  $c$  are the ellipsis semi-axes, and  $\theta$  is defined in Figure 8.

The 2D ellipsoidal crack propagation problem is a reasonable approximation for many actual surface, corner, or internal cracks. Fractographic observations indicate that the successive fronts of those cracks tend to achieve an elliptical form, see Figure 9, and to stay approximately elliptic during their fatigue propagation, even when the initial crack shape is far from an ellipsis [31, 32]. Therefore, it can be quite reasonable to assume in the modeling that the fatigue propagation just changes the shape of the 2D cracks (given by the ratio  $a/c$  between the ellipsis semi-axes, which quantifies how elongated the cracks are), but preserves their basic ellipsoidal geometry.

As an ellipsis is completely defined by its two semi-axes, to predict the growth of 2D (elliptical) cracks, including their shape changes, it is enough to calculate at each load cycle the lengths of the ellipsis axes  $a$  and  $c$ , **jointly** solving the  $da/dN$  and the  $dc/dN$  propagation problems.

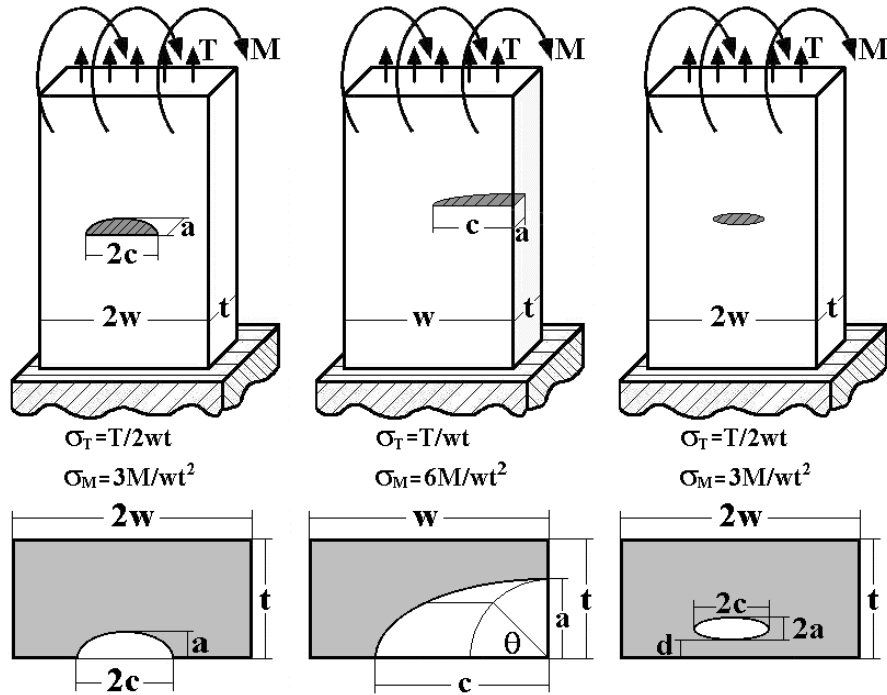


Figure 8 – Surface semi-elliptical, corner quart-elliptical, and internal elliptical cracks.

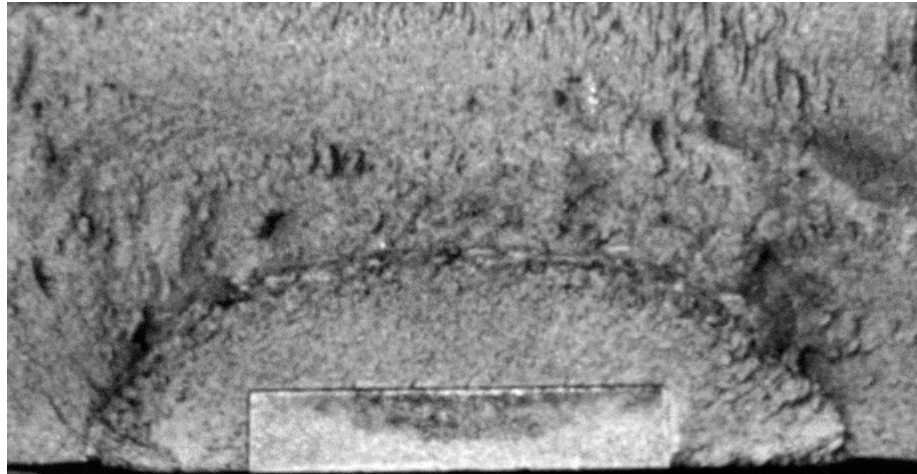


Figure 9 – A surface fatigue crack that started from a sharp rectangular notch and grew with an approximately semi-elliptical front.

To exemplify the simplest case of this type of problem, the semi-elliptical surface crack with  $a < c$  under pure normal loading  $\Delta\sigma$  is briefly analyzed. The expression for  $\Delta K(a) = \Delta\sigma \cdot [\sqrt{\pi a}] f_a(a/c, a/t, c/W)$  from the Newman and Raju solution [29] is quite complex, although the ratio  $\Delta K(a)/\Delta K(c)$  is relatively simple, allowing for the visualization of the basic ideas of the calculation methodology

$$\Delta K(c) = \Delta K(a) \cdot \sqrt{\frac{a}{c}} \cdot [1.1 + 0.35(a/t)^2] \quad (23)$$

The calculation model requires the crack type and initial size  $a_0$  and  $c_0$ , the bar geometry, the loading type, the mechanical properties, and the crack propagation rule  $da/dN = F(\Delta K, R, \Delta K_{th}, K_c, \dots)$  of the material. A small crack increment  $\delta a$  must also be specified (50 $\mu$ m, a number of the order of the resolution threshold of the crack measurement methods in fatigue tests, can be a good choice both from the physical and from the numeric points of view). From the complex loading,  $\Delta\sigma_{rms}$  and  $R_{rms}$  are calculated to obtain

$$\Delta K_{rms}(a_0) = \Delta\sigma_{rms} \cdot [\sqrt{(\pi a_0)} f_a(a_0/c_0, a_0/t, c_0/W)] \quad (24)$$

The number of cycles  $N_0$  the crack takes to grow from  $a_0$  to  $a_0 + \delta a$  is given by

$$N_0 = \frac{\delta a}{F(\Delta K_{rms}(a_0), R_{rms}, \Delta K_{th}, K_c, \dots)} \quad (25)$$

$\Delta K_{rms}(c_0)$  can be calculated by Equation 23, or by an expression similar to Equation 24, to get the correspondent growth in the direction of the semi-axis  $c$ ,  $\delta c_0$ , which is given by

$$\delta c_0 = N_0 \cdot F(\Delta K_{rms}(c_0), R_{rms}, \Delta K_{th}, K_c, \dots) \quad (26)$$

The numerical calculation process can now start the coupled interactions making  $\Delta K_{rms}(a_1) = \Delta K_{rms}(a_0 + \delta a)$  and calculating  $N_1 = \delta a / F(\Delta K_{rms}(a_1), R_{rms}, \Delta K_{th}, K_c, \dots)$ , in order to get  $\delta c_1 = N_1 \cdot F(\Delta K_{rms}(c_1), R_{rms}, \Delta K_{th}, K_c, \dots)$ , where  $c_1 = c_0 + \delta c_0$ , etc. The precision of the methodology can be adjusted by the value of  $\delta a$ .

When compared to the 1D growth, the application of the  $\Delta K_{rms}$  method to the 2D problem is more laborious and uses a less efficient integration method but does not present supplementary conceptual difficulties. However, it should be noticed that the 2D propagation presents some particularities that differentiate it from the 1D case. As these cracks have different values for  $\Delta K(a)$  and  $\Delta K(c)$ , there are three distinct 2D propagation cases under simple loading (assuming  $\Delta K(a) > \Delta K(c)$  to start with)

- 1)  $\Delta K(a_0)$  and  $\Delta K(c_0) > \Delta K_{th}$ : the crack spreads in both directions, changing shape at each  $i$ -th load cycle depending on the ratio  $\Delta K(a_i)/\Delta K(c_i)$ .
- 2)  $\Delta K(a_0) > \Delta K_{th}$  and  $\Delta K(c_0) < \Delta K_{th}$ : the crack grows only in the  $a$  direction, until its size is big enough to make  $\Delta K(c_0) > \Delta K_{th}$ , when the problem reverts to Case 1 (there are, however, pathological cases in which  $\Delta K(a)$  **decreases** with  $a$ , and in these cases a crack can start spreading to later on stop if it reaches  $\Delta K(a) < \Delta K_{th}$ ). Moreover, it is worth mentioning that this Case 2 is particularly deceiving in inspections, since the trace of a surface crack can remain constant during millions of cycles [32], apparently hinting that it is inactive, when in fact it is growing toward the inside of the piece, until reaching  $\Delta K(c_0) > \Delta K_{th}$ , when it starts to spread laterally in a relatively fast rate.
- 3)  $\Delta K(a_0)$  and  $\Delta K(c_0) < \Delta K_{th}$ : the crack does not propagate.



In the complex loading case there are other details to consider. For instance, it is not possible to guarantee 2D crack inactivity if  $\Delta K_{rms}(a_0)$  and  $\Delta K_{rms}(c_0) < \Delta K_{th}$ . But, due to space limitations, the study of these details is left for another work.

To conclude, it is worthwhile remembering that the  $\Delta K_{rms}$  method is the simplest way to treat a complex loading problem, but it should only be used, as with any model, with the due appreciation of its limitations.

### The Cycle-by-Cycle Method

In the cycle-by-cycle method, each load reversion is associated to the crack growth it would cause if it was the only one to load the piece (this implicates neglecting interaction effects among the several events of a complex loading, such as overload-induced retardation or arrest in the crack growth). Using this assumption, it is easy to write a general expression for the cycle-by-cycle crack growth, by any crack propagation rule: if  $da/dN = F(\Delta K, R, \Delta K_{th}, K_C, \dots)$ , and if in the  $i$ -th 1/2 cycle of the loading the length of the crack is  $a_i$ , the stress range is  $\Delta\sigma_i$  and the mean load causes  $R_i$ , then the crack grows by a  $\delta a_i$  given by

$$\delta a_i = \frac{1}{2} \cdot F(\Delta K(\Delta\sigma_i, a_i), R(\Delta\sigma_i, \sigma_{max_i}), \Delta K_{th}, K_C, \dots) \quad (27)$$

The total growth of the crack is quantified by  $\Sigma(\delta a_i)$ . Therefore, the cycle-by-cycle rule is similar in concept to the linear damage accumulation used in the  $SN$  and  $\epsilon N$  fatigue design methods. And, as in Miner's rule, it requests that **all** the events that cause fatigue damage be recognized before the calculation, by rain-flow counting the loading.

However, this counting algorithm alters the **order** of the loading, as shown in Figure 10. This can cause serious problems in the predictions, because the loading order effects in crack propagation are of two different natures.

- Delayed effects can retard or stop the subsequent growth of the crack due, e.g., to plasticity-induced Elber-type crack closure [33] or to crack tip bifurcation. These interaction effects among the loading cycles normally increase the crack life and, if neglected in the calculation, may induce excessively conservative predictions.
- Instantaneous fracture occurs when  $K_{max} = K_C$  in **one** event, which must be precisely predicted.

As already mentioned above, the loading input in the **ViDa** software is sequential, and preserves the time order information that is lost when histograms or any other loading statistics are generated. To take advantage of this feature, a **sequential** rain-flow counting option was introduced in the software (Figure 10). The sequential rain-flow reorders the results from the traditional rain-flow based on the ending point location of each counted range pair [25]. With this technique, the effect of each large loading event is counted when it happens (and not before its occurrence, as in the traditional rain-flow method).

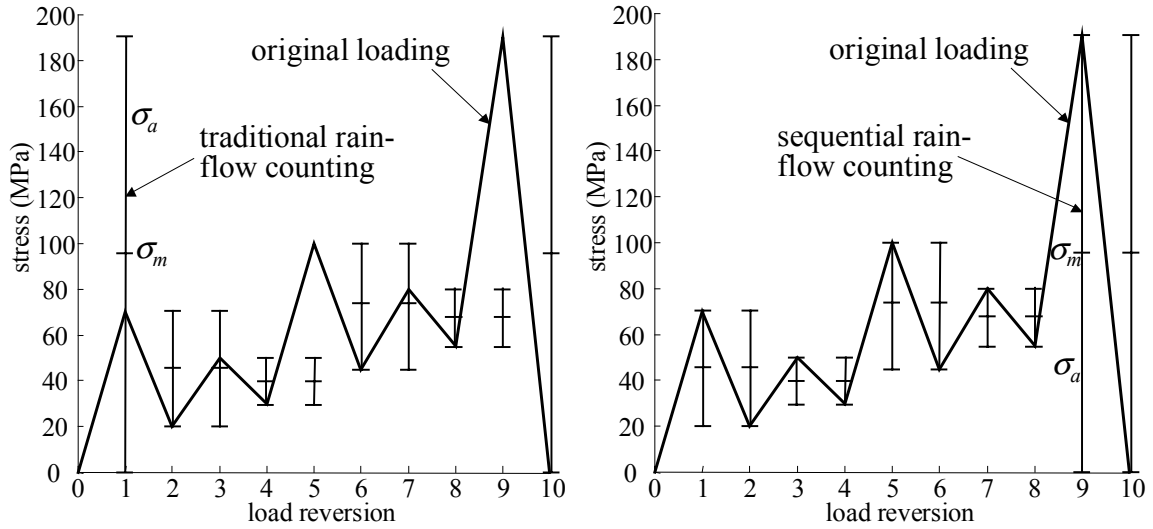


Figure 10 – *Traditional rain-flow counting, anticipating the large load events, and sequential rain-flow counting, which preserves most of the loading order.*

The main advantage of the sequential rain-flow counting algorithm is to avoid the premature calculation of the overload effects, which can cause **non-conservative** crack propagation life predictions (as  $K(\sigma, a)$  in general grows with the crack, a given overload applied when the crack is large can be much more harmful than applied when the crack is small). The sequential rain-flow does not eliminate all the sequencing problems caused by the traditional method, but it is certainly an advisable option because it presents advantages over the original algorithm, without increasing its difficulty.

As discussed in the  $\Delta K_{rms}$  method, the compressive part of the loading can be discarded in the calculations, that is, the negative peaks and valleys can be zeroed before the computations to decrease the numerical effort of the cycle-by-cycle method. And, in the same way, a range filtering option can be very useful to discard small loads that cause no damage inducing  $\Delta K_i < \Delta K_{th}(R_i)$ , following the ideas of the race-track method [34].

The range filtering can indeed significantly reduce the computational effort in fatigue damage calculations if the complex loading history is long. But this procedure is intrinsically **non-conservative**, because it can disregard damaging events as  $\Delta K_i$  is not available before the crack growth calculations ( $\Delta K$  depends not only on the loads, but also on the size of the crack). In consequence, the conservative rule is to limit the cut of the loading to the pairs  $(\Delta\sigma_i, R_i)$  that cause  $\Delta K(a_f) < \Delta K_{th}[R(a_f)]$ , where  $a_f$  is the expected final length for the crack. But, in practice it can be easier numerically to try decreasing the ranges for the filtering, until there is no significant variation in the results.

The computational implementation of Equation 27, even with the pre-zeroing of the compressive peaks and valleys and with the range filtering of the loading, is still not numerically efficient. For this reason, an additional feature to reduce the computational time can be quite useful: the option of maintaining the geometrical part of  $\Delta K$  constant during small variations in crack size.

As  $\Delta K = \Delta\sigma \cdot [\sqrt{\pi a}] \cdot f(a/W)$ , where  $f(a/W)$  is a non-dimensional function (usually complicated) that depends only on the piece and crack geometry and not on the loading, it

can be said that the range of the stress intensity factor  $\Delta K_i$  at each load reversion depends on two variables of different nature:

1. on the stress range  $\Delta\sigma_i$  in that event, and
2. on the length of the crack  $a_i$  in that instant.

$\Delta\sigma_i$ , of course, can vary significantly at each load reversion when the loading is complex, but fatigue cracks always grow very slowly. In fact, at least in structural metals, the largest rates of stable crack growth observed in practice are of the order of  $\mu\text{m}/\text{cycle}$ , and during most of the life the crack growth rates are better measured in  $\text{nm}/\text{cycle}$ .

However, as in general the usually complicated  $f(a/W)$  expressions do not present discontinuities, one can take advantage of the small changes in  $f(a/W)$  during small increments in crack length. In this way, instead of calculating at each load cycle the value of  $\Delta K_i = \Delta\sigma_i \cdot [\sqrt{(\pi a_i)} \cdot f(a_i/W)]$ , a task that demands great computational effort, it is more efficient to hold  $f(a_i/W)$  constant during a (small) percentage of crack increment  $\delta a\%$ , that should be specifiable by the calculation software user. The errors introduced by this procedure are non-conservative, but they decrease quickly with the value specified for  $\delta a\%$ . Convergence is assumed when decreasing values of  $\delta a\%$  do not influence significantly the calculated crack growth. In practice,  $\delta a\%$  values of the order of  $0.5\%$  result in adequate predictions for most calculations [25].

#### *Two-Dimensional Crack Growth by the Cycle-by-Cycle Method*

The 2D growth of elliptical cracks problem can be treated in manner similar to that already discussed in the  $\Delta K_{rms}$  method: if in the  $i$ -th loading event the ellipsoidal crack has semi-axes  $a_i$  and  $c_i$ , under

$$\Delta K(a_i) = \Delta\sigma_i \cdot [\sqrt{(\pi a_i)} \cdot f_a(a_i/c_i, a_i/t, c_i/W)] \text{ and } \Delta K(c_i) = \Delta\sigma_i \cdot [\sqrt{(\pi a_i)} \cdot f_c(a_i/c_i, a_i/t, c_i/W)] \quad (28)$$

stress intensity ranges, and if  $da/dN = F(\Delta K, R, \Delta K_{th}, K_C, \dots)$  is the crack growth rule of the material, then the crack increment in this  $i$ -th 1/2 cycle is given by

$$\delta a_i = \frac{1}{2} \cdot F(\Delta K(\Delta\sigma_i, a_i, f_a), R(\Delta\sigma_i, \sigma_{max_i}), \Delta K_{th}, K_C, \dots) \quad (29)$$

$$\delta c_i = \frac{1}{2} \cdot F(\Delta K(\Delta\sigma_i, a_i, f_c), R(\Delta\sigma_i, \sigma_{max_i}), \Delta K_{th}, K_C, \dots) \quad (30)$$

The crack growth is calculated by the simultaneous solution of  $\Sigma\delta a_i$  and  $\Sigma\delta c_i$ . As the crack increments  $\delta a_i$  and  $\delta c_i$  depend on both  $a_i$  and  $c_i$ , the coupled 2D growth is well characterized.

It is worth mentioning that all the comments made above about the filtering and the counting of the loading can be also applied to 2D crack growth. In the same way, the maintenance of  $f_a$  and  $f_c$  constant during a small  $\delta a\%$  (or  $\delta c\%$ ) variation in crack length is still more useful in 2D calculations, because the analytical expressions for  $f_a$  and  $f_c$  are generally very complex, and demand great numerical effort. But, besides the

computational complexity, the 2D cycle-by-cycle problem does not present significant supplementary conceptual difficulties over the 1D case.

### **Load Cycle Interaction Effects**

It is a well-known fact that interaction problems among load cycles can have a very significant effect in the prediction of fatigue crack growth. There is a vast literature proving that tensile overloads, when applied over a loading whose amplitude otherwise stays constant, can cause retardation or arrest in the crack growth, and that even compressive overloads can sometimes affect the rate of subsequent crack propagation [33, 35, 36].

Neglecting these effects in fatigue life calculations can completely invalidate the predictions. In fact, only after considering overload induced retardation effects can the life reached by real structural components be justified when modeling many practical problems. However, the generation of an universal algorithm to quantify these effects is particularly difficult, due to the number and to the complexity of the mechanisms involved in fatigue crack retardation, among them: plasticity-induced crack closure; blunting and/or bifurcation of the crack tip; residual stresses and/or strains; strain-hardening; crack face roughness, and oxidation of the crack faces.

Besides, depending on the case, several of these mechanisms may act concomitantly or competitively, as a function of factors such as: size of the crack; microstructure of the material; dominant stress state, and environment.

The detailed discussion of this complex phenomenology is considered beyond the scope of this work (a revision of the phenomenological problem can be found in [33]). Moreover, the relative importance of the several mechanisms can vary from case to case, and there is, so far, no universally accepted single equation capable of describing the whole problem. Therefore, from the designer's point of view it must necessarily be treated in the most reasonably simplified way.

A simplified model can not be unrealistic so it is worthwhile mentioning that some simplistic models are unacceptable. For example, attributing the overloads to a significant variation in the residual stress state **at** the crack tip in order to justify the retardation effects is not reasonable. This is mechanically impossible: the tensile yielding during the loading and the compressive yielding during the unloading close to the crack tip during fatigue crack propagation prevent any significant variation in the residual stress state **at** the crack tip after an overload. On the other hand, the principal characteristic of fatigue cracks is to propagate cutting a material that has already been deformed by the plastic zone that always accompanies their tips. In this way, the fatigue crack faces are embedded in an envelope of (plastic) residual strains and, consequently, they compress their faces when completely discharged, and they open alleviating in a progressive way the (compressive) load transmitted through their faces.

According to Elber [37], only after completely opening the crack at a load  $K_{op}$ , would the crack tip be stressed. Therefore, the bigger the  $K_{op}$ , the less would be the effective stress intensity range  $\Delta K_{eff} = K_{max} - K_{op}$ , and this  $\Delta K_{eff}$  instead of  $\Delta K$  would be the crack propagation rate controlling parameter. Most load interaction models are, although indirectly, based in this idea. This implicates in the supposition that the principal retardation mechanism is caused by plasticity induced crack closure: in these cases, the

opening load should **increase** when the crack penetrates into the plastic zone inflated by the overload, **reducing** the  $\Delta K_{eff}$  and stopping or delaying the crack, while the plastic zones associated with the loading are contained in the overload induced plastic zone.

It is very important to emphasize that this is by no means the only mechanism that can induce crack retardation. For example, Castro and Parks [38] showed that, under dominant plane strain conditions, overload induced fatigue crack retardation or arrest can occur while  $\Delta K_{eff}$  **increases**. The principal retardation mechanism in those cases was bifurcation of the crack tip.

The Wheeler model is the most popular retardation model [35]. The model is simplistic and assumes, more or less arbitrarily, that while the loading plastic zone  $ZP_i$  is embedded in the overload plastic zone  $ZP_{ov}$ , the crack growth rate retardation depends on the distance from the border of  $ZP_{ov}$  to the tip of the crack, see Figure 11.

The retardation is maximum just after the overload, and stops when the border of  $ZP_i$  touches the border of  $ZP_{ov}$ . Therefore, if  $a_{ov}$  and  $a_i$  are the crack sizes at the instant of the overload and at the  $i$ -th cycle, and  $(da/dN)_{reti}$  and  $(da/dN)_i$  are the retarded and the non-retarded crack growth rate (at which the crack would be growing in the  $i$ -th cycle if the overload had not occurred), then, according to Wheeler

$$\left(\frac{da}{dN}\right)_{ret_i} = \left(\frac{da}{dN}\right)_i \cdot \left(\frac{ZP_i}{a_{ov} + ZP_{ov} - a_i}\right)^\beta, \quad a_i + ZP_i < a_{ov} + ZP_{ov} \quad (31)$$

where  $\beta$  is an experimentally adjustable constant. Broek [35, 36] mentions Wheeler's data for steels ( $\beta = 1.43$ ) and for Ti-6AL-4V ( $\beta = 3.4$ ), and suggests that other typical values for  $\beta$  are between 0 and 2.

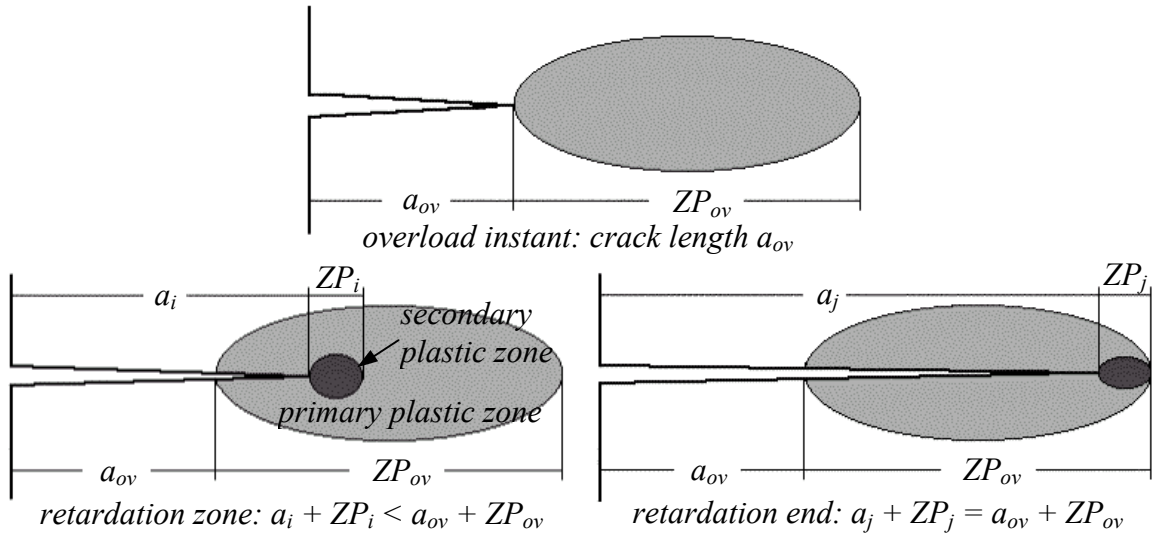


Figure 11 – Wheeler crack growth retardation model.

It should be noticed that this model cannot predict crack arrest that has been observed. As  $ZP \approx (K_{max}/S_Y)^2$ , where  $S_Y$  is the yielding strength of the material, the maximum value

of the predicted retardation happens immediately after the overload, and is equal to  $(K_{max}/K_{ov})^{2\beta}$ , where  $K_{max}$  is the maximum load in the cycle just after the overload, and  $K_{ov}$  is the overload peak. Therefore, the phenomenology of the load cycle interaction problem is not completely reproducible by the Wheeler original model. However, also to model crack arrest, a simple modification that seems reasonable is to use a Wheeler-like parameter to multiply  $\Delta K$  instead of  $da/dN$  after the overload

$$\Delta K_{ret}(a_i) = \Delta K(a_i) \cdot \left( \frac{ZP_i}{a_{ov} + ZP_{ov} - a_i} \right)^\gamma, \quad a_i + ZP_i < a_{ov} + ZP_{ov} \quad (32)$$

where  $\Delta K_{ret}(a_i)$  and  $\Delta K(a_i)$  are the values of the stress intensity factors that would be acting at  $a_i$  with and without retardation due to the overload, and  $\gamma$  is in general different from the original model exponent  $\beta$ . This simple modification can be used with any of the propagation rules that recognize  $\Delta K_{th}$  to predict both the retardation and the stop of fatigue cracks after an overload (the stop occurring if  $\Delta K_{ret}(a_i) < \Delta K_{th}$ ).

The numeric implementation of these retardation models in a cycle-by-cycle algorithm is not conceptually difficult, but it requires a considerable programming effort. To illustrate the main ideas, a simplified flow-chart of the calculation algorithm used in the **ViDa** software is shown in Figure 12.

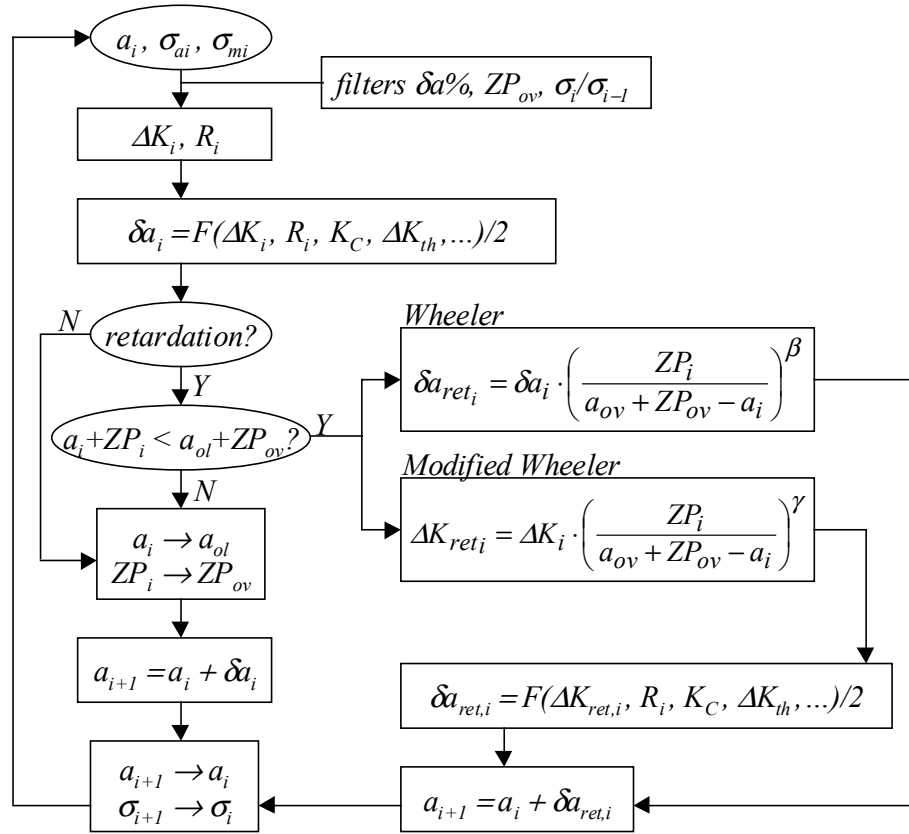


Figure 12 – Simplified flow-chart of the calculation algorithm used in the **ViDa** software to predict fatigue crack propagation under complex loading.

Some calculation details are worth mentioning. The first one refers to the use of the  $\delta\alpha\%$  filter, since crack size increments that work well otherwise can cause troubles with the retardation models, as the plastic zone sizes can be very small compared to the crack size. In order to quantify the propagation gradient inside the overload affected zone,  $\delta\alpha\%$  must be much smaller than  $ZP_{ov}$ .

A second one can save a lot of computational time when the loading is complex. Small variations in the loading amplitude do not cause experimentally detectable crack retardation, and they should not be considered as overloads in the calculation model. Therefore, a numerical filter for overloads can be profitably introduced in the algorithm, specifying that there is no overload effect if  $\sigma_j/\sigma_{j-1} < \alpha$ , where  $\sigma_{j-1}$  and  $\sigma_j$  are successive peaks of the loading and  $\alpha$  is an adjustable constant (that, in the absence of better information, can be chosen as 1.25 or 1.3).

There are several other retardation models [33, 39], but none of those that can be implemented in a local approach code has definitive advantages over the simpler Wheeler models discussed above. This is no surprise, since single equations are too simplistic to model all the several mechanisms that can induce retardation effects. Therefore, in the same way that a curve  $da/dN$  vs.  $\Delta K$  is experimentally measured, a propagation model can be adjusted to experimental data to calibrate the exponents of Equations 31 or 32, as recommended by Broek [35].

Using these same concepts, it is not particularly difficult to model retardation effects in 2D crack propagation. The idea is to maintain the fundamental hypothesis of the ellipsoidal geometry preservation, accounting for the coupled growth of the semi-axes  $a$  and  $c$ . However, as the size of the plastic zones depends on the value of  $\Delta K$ , and as in general  $\Delta K(a) \neq \Delta K(c)$ , the retardation effects in 2D growth can be different in each direction. Thus, after each overload the value of  $\Delta K_{ret}(a_i)$  and  $\Delta K_{ret}(c_i)$  are calculated by

$$\Delta K_{ret}(a_i) = \Delta K(a_i) \cdot \left( \frac{ZP(a_i)}{a_{ov} + ZP(a_{ov}) - a_i} \right)^\gamma, \quad a_i + ZP(a_i) < a_{ov} + ZP(a_{ov}) \quad (33)$$

$$\Delta K_{ret}(c_i) = \Delta K(c_i) \cdot \left( \frac{ZP(c_i)}{c_{ov} + ZP(c_{ov}) - c_i} \right)^\gamma, \quad c_i + ZP(c_i) < c_{ov} + ZP(c_{ov}) \quad (34)$$

From these values, it is easy to calculate the crack growth in the two elliptic semi-axes directions during the  $i$ -th 1/2 cycle of the loading

$$\delta a_i = \frac{1}{2} \cdot F(\Delta K_{ret}(\Delta\sigma_i, a_i, f_a), R(\Delta\sigma_i, \sigma_{max_i}), \Delta K_{th}, K_c, \dots) \quad (35)$$

$$\delta c_i = \frac{1}{2} \cdot F(\Delta K_{ret}(\Delta\sigma_i, a_i, f_c), R(\Delta\sigma_i, \sigma_{max_i}), \Delta K_{th}, K_c, \dots) \quad (36)$$

Only the modified Wheeler model is presented above, but it is trivial to write similar equations for the original model. Finally, it should be mentioned that all the filtering remarks already discussed are also applied to the 2D case.

## Conclusions

In this paper, a two-phase methodology was presented to predict fatigue crack propagation in generic 2D structures under complex loading. First, self-adaptive finite-elements were used to calculate, by three different methods, the fatigue crack path and the stress intensity factors along the crack length  $K_I(a)$  and  $K_{II}(a)$ , at each propagation step. The calculated  $K_I(a)$  was then used to predict the propagation fatigue life of the structure by the local approach, using the root mean square or the cycle-by-cycle integration methods, even considering overload-induced crack retardation effects in this latter one. Two complementary software programs were developed to implement this methodology. The first software package is an interactive graphics program for simulating two-dimensional fracture processes based on a finite element adaptive mesh generation strategy. The second is general purpose fatigue design software developed to predict both initiation and propagation fatigue lives under complex loading by all classical design methods. In particular, its crack propagation module accepts any stress intensity factor expressions, including the ones generated by the finite-element software. Experimental results showed that the presented methodology and its software implementation could effectively predict fatigue crack propagation in an arbitrary two-dimensional structural component.

## References

- [1] Shih, C.F., de Lorenzi, H.G., and German, M.D., "Crack Extension Modeling with Singular Quadratic Isoparametric Elements," *International Journal of Fracture*, Vol. 12, 1976, pp. 647-651.
- [2] Rybicki, E.F. and Kanninen, M.F., "A Finite Element Calculation of Stress-Intensity Factors by a Modified Crack Closure Integral," *Engineering Fracture Mechanics*, Vol. 9, 1977, pp. 931-938.
- [3] Raju, I.S., "Calculation of Strain-Energy Release Rates with Higher Order and Singular Finite Elements," *Engineering Fracture Mechanics*, Vol. 28, 1987, pp. 251-274.
- [4] Bui, H.D. "Associated Path Independent J-Integrals for Separating Mixed Modes," *Journal of Mechanics & Physics Solids*, Vol. 31, 1983, pp. 439-448.
- [5] Dodds, R.H. Jr. and Vargas, P.M., "Numerical Evaluation of Domain and Contour Integrals for Nonlinear Fracture Mechanics," Report UILU-ENG-88-2006, Dept. of Civil Engineering, University of Illinois, Urbana-Champaign, 1988.
- [6] Banks-Sills, L. and Sherman, D., "Comparison of Method for Calculating Stress-Intensity Factors with Quarter-Point Elements," *International Journal of Fracture Mechanics*, Vol. 32, 1986, pp. 127-140.
- [7] Nikishkov, G.P. and Atluri, S.N., "An Equivalent Domain Integral Method for Computing Crack-Tip Integral Parameters in Non-Elastic Thermo-Mechanical Fracture," *Engineering Fracture Mechanics*, Vol. 26, 1987, pp. 851-867.



- [8] Chen, K.L. and Atluri, N. "Comparison of Different Methods of Evaluation of Weight Functions for 2D Mixed-Mode Fracture Analysis," *Engineering Fracture Mechanics*, Vol. 34, 1989, pp. 935-956.
- [9] Rice, J.R., "A Path Independent Integral and the Approximate Analysis of Strain Concentration by Notches and Cracks," *Journal of Applied Mechanics*, Vol. 35, 1968, pp. 379-386.
- [10] Knowles, J.K. and Sternberg, E., "On a Class of Conservation Laws in Linearized and Finite Elastostatics," *Archives for Rational Mechanics & Analysis*, Vol. 44, 1972, pp. 187-211.
- [11] Atluri, S.N., "Path-Independent Integrals in Finite Elasticity and Inelasticity, with Body Forces, Inertia, and Arbitrary Crack-Face Conditions," *Engineering Fracture Mechanics*, Vol. 16, 1982, pp. 341-369.
- [12] Eischen, J.W., "An Improved Method for Computing the J2 Integral," *Engineering Fracture Mechanics*, Vol. 26, 1987, pp. 691-700.
- [13] Kienzler, R. and Kordisch, H., "Calculation of J1 and J2 Using the L and M Integrals," *International Journal of Fracture*, Vol. 43, 1990, pp. 213-225.
- [14] Erdogan, F. and Sih, G.C., "On the Crack Extension in Plates under Plane Loading and Transverse Shear," *Journal of Basic Engineering*, Vol. 85, 1963, pp. 519-527.
- [15] Hussain, M.A., Pu, S.U., and Underwood, J., "Strain Energy Release Rate for a Crack under Combined Mode I and II," *ASTM STP 560*, 1974, pp. 2-28.
- [16] Sih, G.C., "Strain-Energy-Density Factor Applied to Mixed Mode Crack Problems," *International Journal of Fracture Mechanics*, Vol. 10, 1974, pp. 305-321.
- [17] Bittencourt, T.N., Wawrzynek, P.A., Ingraffea, A.R., and Sousa, J.L.A., "Quasi-Automatic Simulation of Crack Propagation for 2D LEFM Problems," *Engineering Fracture Mechanics*, Vol. 55, 1996, pp. 321-334.
- [18] Barsom, J.M. and Rolfe, S.T., *Fracture and Fatigue Control in Structures*, Prentice-Hall, New Jersey, 1987.
- [19] Araújo, T.D.P. "Adaptive Simulation of Elastic-Plastic Fracturing," (in Portuguese), PhD dissertation, Department of Civil Engineering, Pontifical Catholic University of Rio de Janeiro (PUC-Rio), Brazil, 1999.
- [20] Carvalho, C.V., Araújo, T.D.P., Cavalcante, J.B., Martha, L.F., and Bittencourt, T.N., "Automatic Fatigue Crack Propagation using a Self-adaptive Strategy," *PACAM VI - Sixth Pan-American Congress of Applied Mechanics*, Rio de Janeiro, Vol. 6, 1999, pp. 377-380.
- [21] Paulino, G.H., Menezes, I.F., Cavalcante, J.B., and Martha, L.F., "A Methodology for Adaptive Finite Element Analysis: Towards an Integrated Computational Environment," *Computational Mechanics*, Vol. 23, 1999, pp. 361-388.

- [22] Araújo, T.D.P., Cavalcante, J.B., Carvalho, M.T.M., Bittencourt, T.N., and Martha, L.F., "Adaptive Simulation of Fracture Processes Based on Spatial Enumeration Techniques," *International Journal the Rock Mechanics and Mining Sciences*, Vol. 34, 1997, p. 551 (abstract) and CD-ROM Paper No. 188 (full paper).
- [23] Baehmann, P.L., Wittchen, S.L., Shephard, M.S., "Robust Geometrically Based, Automatic Two-Dimensional Mesh Generation," *International Journal for Numerical Methods in Engineering*, Vol. 24, 1987, pp. 1043-1087.
- [24] de Floriani, L., and Puppo, E., "An On-line Algorithm for Constrained Delaunay Triangulation," *Graphical Models and Image Processing*, Vol. 54, 1992, pp. 290-300.
- [25] Meggiolaro, M.A. and Castro, J.T.P., "**ViDa 98** – a Visual Damagemeter to Automatize the Fatigue Design under Complex Loading," (in Portuguese), *Revista Brasileira de Ciências Mecânicas*, Vol. 20, 1998, pp. 666-685.
- [26] Castro, J.T.P. and Meggiolaro, M.A., "Some Comments on the  $\epsilon N$  Method Automation for Fatigue Dimensioning under Complex Loading," (in Portuguese), *Revista Brasileira de Ciências Mecânicas*, Vol. 21, 1999, pp. 294-312.
- [27] Hudson, C.M., "A Root-Mean-Square Approach for Predicting Fatigue Crack Growth under Random Loading," *ASTM STP 748*, 1981, pp. 41-52.
- [28] Newman, J.C., "A Review and Assessment of the Stress Intensity Factors for Surface Cracks," *ASTM STP 687*, 1979, pp. 16-46.
- [29] Newman, J.C. and Raju, I.S., "Stress-Intensity Factor Equations for Cracks in Three-Dimensional Finite Bodies Subjected to Tension and Bending Loads," NASA TM-85793, 1984.
- [30] Anderson, T.L. *Fracture Mechanics*, CRC, 1995.
- [31] Castro, J.T.P., Giassone, A., and Kenedi, P.P., "Fatigue Propagation of Superficial Cracks in Wet Welds," *Fracture, Fatigue and Life Prediction*, 1995, pp. 21-38.
- [32] Castro, J.T.P., Giassoni, A., and Kenedi, P.P., "Fatigue Propagation of Semi and Quart-Elliptical Cracks in Wet Welds," (in Portuguese), *Revista Brasileira de Ciências Mecânicas*, Vol. 20, 1998, pp. 263-277.
- [33] Suresh, S., *Fatigue of Materials*, Cambridge, 1998.
- [34] Nelson, D.V. and Fuchs, H.O., "Predictions of Cumulative Fatigue Damage Using Condensed Load Histories," in *Fatigue Under Complex Loading*, SAE, 1977.
- [35] Broek, D., *The Practical Use of Fracture Mechanics*, Kluwer 1988.
- [36] Broek, D., *Elementary Engineering Fracture Mechanics*, Martinus Nijhoff 1986.
- [37] Elber, W., "The Significance of Fatigue Crack Closure," *ASTM STP 486*, 1971.
- [38] Castro, J.T.P. and Parks, D.M., "Decrease in Closure and Delay of Fatigue Crack Growth in Plane Strain," *Scripta Metallurgica*, Vol. 16, 1982, pp. 1443-1445.
- [39] Chang, J.B and Hudson, C.M. ed., *Methods and Models for Predicting Fatigue Crack Growth Under Random Loading*, *ASTM STP 748*, ASTM, 1981.